The role of high molecular weight chains in flow-induced crystallization precursor structures

2006 J. Phys.: Condens. Matter 18 S2421

(http://iopscience.iop.org/0953-8984/18/36/S15)

INSTITUTE OF PHYSICS PUBLISHING JOURNAL OF PHYSICS: CONDENSED MATTER

J. Phys.: Condens. Matter **18** (2006) S2421–S2436 doi:10.1088/0953-8984/18/36/S15

The role of high molecular weight chains in flow-induced crystallization precursor structures

Ling Yang[1], Rajesh H Somani[1], Igors Sics[1], Benjamin S Hsiao[1,4], Rainer Kolb[2] and David Lohse[3]

[1] Department of Chemistry, Stony Brook University, Stony Brook, NY 11794-3400, USA
[2] ExxonMobil Chemical Company, Univation Technologies, Baytown, TX 77520, USA
[3] ExxonMobil Research and Engineering Company, Annandale, NJ 08801, USA

E-mail: bhsiao@notes.cc.sunysb.edu

Received 31 January 2006, in final form 12 July 2006
Published 24 August 2006
Online at stacks.iop.org/JPhysCM/18/S2421

Abstract

Flow-induced crystallization in a bimodal polyethylene blend was investigated by means of *in situ* shear-WAXD (wide-angle x-ray diffraction) and shear-SAXS (small-angle x-ray scattering) techniques. The blend contained a low molecular weight (M_w = 50 000 g mol^{-1} and polydispersity = 2) polyethylene copolymer matrix (MB-50k) with 2 mol% of hexene, and a nearly monodisperse high molecular weight (M_w = 161 000 g mol^{-1} and polydispersity = 1.1) hydrogenated polybutadiene component (MD-161k), which has the microstructure of an ethylene–butene copolymer with 4 mol% butene. At the experimental temperatures of 112 and 115 °C, MB-50k exhibited faster crystallization kinetics and higher crystallinity due to higher chain mobility and higher ethylene content than those of the MB-50k/MD-161k blend. However, both WAXD and SAXS results indicated that the high molecular weight component (MD-161k) is responsible for the formation of more highly oriented crystals, which we relate to a shear-induced precursor scaffold. Values of the lamellar long period in all experimental runs were found to slightly decrease in the beginning of crystallization and then reached a plateau value. Vonk's method for single lamella scattering was employed to estimate the lamellar thickness in the MB-50k/MD-161k blend at high temperature (115 °C), where the lamellar thickness was also found to decrease in the beginning and remained about constant afterward. Twisted lamellar structures were observed in all formed kebabs.

[4] Author to whom any correspondence should be addressed.

1. Introduction

External flow causes extension and orientation of polymer chains, which leads to the formation of crystallization precursor structures. Many studies [1–9] indicated that the crystallization behaviour and subsequent morphological development are directly dictated by the initially formed precursor structures (e.g. shish-kebab structures, where shish represents extended-chain crystal and kebab represents folded-chain crystal) induced by flow. Understanding of the exact nature of the crystallization precursor structures under flow can allow us to control the morphology and end properties of polymer products, and thus is extremely important from both scientific and technological points of view.

Recently, extensive experimental and simulation efforts have been made to investigate the role of long chain species in the formation of crystallization precursor structures. The chain dynamics has been recognized as the critical process in such formation. Since the relaxation time is proportional to the molecular weight, long chains would possess much longer relaxation times than short chains. As a result, after the cessation of flow, long polymer chains may not have sufficient time to relax back to the coiled state and would remain in the stretched state, whereas short chains can quickly relax back to the coiled state without preferred orientation. Keller [1] proposed that only those polymer chains with molecular weights greater than a critical value could undergo the *coil-stretch* transition and remain oriented, which can result in formation of extended-chain primary nuclei. In contrast, the shorter chains with molecular weights less than the critical value would return to their original coiled state upon relaxation. This critical value was termed as the 'critical orientation molecular weight' (M^*). The concept of M^* in both dilute polymer solutions and entangled polymer melts has been discussed in detail in several previous publications [1, 10–17].

Keller *et al* observed that the shish-kebab structure occurred in both dilute polymer solutions and polymer melts when the systems contained high molecular weight chains [1, 18]. They demonstrated that the addition of one percent of high molecular weight chains could dramatically increase the number of shish-kebab structures in polymer melts under elongational flow [18]. Janeschitz-Kriegl *et al* [19] reported that in short term shearing at a low degree of supercooling, the crystallization of isotactic polypropylene (iPP) was highly dependent on the concentration of long chains. In the presence of long chains, shear-induced crystallization was more sensitive to shear treatment and the orientation of surface layers was much higher than the materials without them. Recently, Kornfield *et al* [20] investigated the blends of two iPP samples with different molecular weight, polydispersity and stereoregularity under a step-shear flow. Their results showed that both crystallization orientation and kinetics increased with increasing long chain content. They argued that the role of long chains in shear-induced crystallization is cooperative rather than a single chain event based on the observation that the oriented structure changed drastically near the overlap concentration of the long chains in binary iPP blends [21]. Several other groups, using similar techniques but under different flow conditions, also reported that the presence of long chains strongly affected the crystallization kinetics and the formation of oriented structures [22–24].

The recent advances in the subject of flow-induced crystallization can be attributed to the availability of several new experimental techniques, such as *in situ* shear-SAXS (small-angle x-ray scattering), shear-WAXD (wide-angle x-ray diffraction), *ex situ*/*in situ* AFM (atomic force microscopy) and TEM (transmission electron microscopy). In addition, computer simulation has also become an important tool for understanding the nature of the initial stage in crystallization (e.g., the formation of nuclei) under flow. For example, the simulation study by Hu *et al* [25] demonstrated that even a single chain could induce transcrystallization under flow. Another simulation by Muthukumar *et al* [26] showed that, even for monodisperse

chains, two populations of chain conformations in the stretched and coiled state can be formed at a given flow rate. The stretched (extended) chains can crystallize into shish, while the coiled chains can form folded-chain lamellae and be adsorbed onto the shish to form kebabs. More recently, in another simulation by Hu *et al* [27], the relaxation of extended chains and subsequent isothermal crystallization of a relaxed melt after flow were studied by means of dynamic Monte Carlo simulations of lattice-polymer chains. They reported that in a binary blend of different chain lengths, the crystallization of oriented long chains acted as the precursor to induce epitaxial crystallization of the relaxed short chains. In other words, the relaxation behaviour of the long-chain component dictated the process of the precursor formation under flow.

Over the past several years, our research group has devoted a great deal of effort to investigate the subject of the initial stage of crystallization in polymer melts induced by step shear using synchrotron x-ray techniques [10–17, 28, 29]. Among these studies, several binary blends were investigated, including the blends of low and high molecular weight polyethylenes [14, 15], blends of low molecular iPP and high molecular weight amorphous atactic PP [17] and blends of iPP and ultra-high molecular weight polyethylene (UHMWPE) [28]. Experimental results from these studies all suggested the important role of the longer chains in forming flow-induced precursor structures, which were responsible for the subsequent development of full-scale crystallization of shorter chains upon cooling. It should be noted that all tested polymer components (either the low molecular weight matrix or the high molecular weight additive) in the above studies had relatively broader molecular weight distributions (polydispersity $\geqslant 2$). The limitation of the broad polydispersity has hindered our current simulation effort to correlate the structure and chain dynamics from the rheological standpoint.

In this work, we have extended the previous studies of binary polyethylene blends. Inspired by Muthukumar's simulation work on monodisperse polymer chains [26], a model blend system, comprised of a low molecular weight polymer matrix (MB-50k) and a small amount of nearly monodispersed high molecular weight polymer additive (MD-161k), was chosen (the two components are fully miscible). In this work, the molecular weight of the minor component was about three times that of the matrix, but marked orientation enhancement was observed in the blend when compared to the matrix. We have extended the current work to include the addition of nearly monodisperse and higher molecular weight components and the results have already been published elsewhere [30]. The blend in this study was deformed under a simple shear flow. *In situ* SAXS and WAXD techniques were utilized to study the structural and morphological development upon cessation of flow. Results from both MB-50k and MB-50k/MD-161k blend were compared to elucidate the role of long chain species on the formation of crystallization precursor structures during flow.

2. Experimental details

2.1. Materials

The low molecular weight polymer was synthesized by metallocene catalyst at ExxonMobil Research and Engineering Company. The sample was a polyethylene copolymer, containing 2 mol% of hexene as the comonomer unit. It had a weight-average molecular weight ($\bar{M}_w$) of about 50 000 g mol^{-1} and a polydispersity of about 2. The high molecular weight additive was prepared by hydrogenation of an anionically synthesized polybutadiene, containing 8% vinyl groups. As such, it had the structure of an ethylene–butene copolymer with 8 wt% (or 4 mol%) butene. This sample was designated as MD-161k as it had an $\bar{M}_w$ about 161 000 g mol^{-1}

Table 1. Molecular weight and melting temperature information of MB-50k and MD-161k, where $\bar{M}_w$ and MWD ($\bar{M}_w/\bar{M}_n$) represent the weight average molecular weight and the molecular weight distribution, respectively; T_m and T_m^{end} represent the nominal melting point and the end position of the endothermic melting peak in DSC measurements.

Samples	$\bar{M}_w$ (g mol^{-1})	MWD ($\bar{M}_w/\bar{M}_n$)	T_m (°C)	T_m^{end} (°C)	T_c (°C)
MB-50k[a]	50 000	2.0	112.2	119.1	98.4
MD-161k[b]	161 000	1.1	108.3	113.2	93.6
MB-50k/MD-161k (90/10)	—	—	112.3	119.0	98.3

[a] Polymerized with 2 mol% of hexene comonomer using the metallocene catalyst method.
[b] Hydrogenated polybutadiene with 8 wt% of 1,2 polybutadiene.

and a polydispersity about 1.1. Although this sample was linear and possessed a narrow molecular weight distribution, the higher degree of short chain branching significantly hindered its crystallization rate when compared to that of MB-50k. The characteristics of these two polymers such as molecular weight information and nominal melting temperature (T_m) and crystallization temperature (T_c) are listed in table 1.

A bimodal polymer blend was prepared by solution blending to ensure intimate mixing of different species at the molecular level. The concentration of the high molecular weight species was 10 wt%. The detailed blending procedure has been described in a previous publication [14]. Polymer films of 0.5–0.7 mm thickness were prepared by compression moulding at 150 °C. Samples in the form of a ring (inner diameter = 10 mm, outer diameter = 20 mm) were cut from the moulded films for shear experiments.

2.2. Experimental procedures

Differential scanning calorimetry (DSC) measurements were carried out to characterize the thermal properties of the blend using a Perkin-Elmer DSC 7 instrument. Two-dimensional (2D) wide-angle x-ray diffraction (WAXD) and small-angle x-ray scattering (SAXS) measurements (not measured simultaneously) were carried out at the X3A2 beamline in the National Synchrotron Light Source (NSLS), Brookhaven National Laboratory (BNL). The wavelength of the synchrotron radiation was 1.54 Å. The shear stage was placed perpendicular to the incident x-ray beam. 2D WAXD and SAXS patterns were collected by means of a MAR CCD x-ray detector (MARUSA) with a resolution of 1024 × 1024 pixels (pixel size = 158.44 μm). The sample-to-detector distance was 98 mm for WAXD and 1690 mm for SAXS. The SAXS angle was calibrated with AgBe (silver behenate) and the WAXD angle was calibrated with Al_2O_3 (aluminium oxide).

In *in situ* shear-x-ray experiments, the polymer sample (in a ring shape) was mounted between two x-ray windows in a modified Linkam CSS-450 shear unit. One window was a Kapton film and another window was a diamond disc. The x-ray beam first went through the diamond window, then the sample, and finally the Kapton film. The gap between the two windows defined the sample thickness. Samples were fully sealed between two plates encapsulating the windows. No sample leaking or shape change occurred after step shearing at high temperature. Shear was applied to the sample by rotating the bottom window while keeping the top window stationary. The mechanical design and electronics of the Linkam stage provided precise control over the various parameters of the shear experiment, including sample thickness, temperature, heating/cooling rate, shear rate, shear strain and duration, as well as the shear mode such as steady, step and oscillatory. The details of the modified Linkam CSS0-450 used for *in situ* x-ray measurements have been introduced in a previous publication [11].

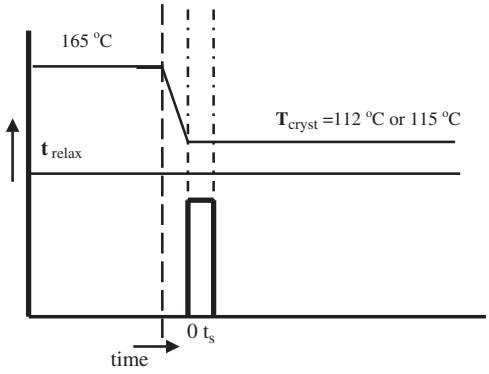

Figure 1. Temperature and shear protocols used for the *in situ* SAXS and WAXD measurements.

In order to ensure that the polymer melt was free of any memory effects associated with clusters or crystal aggregates due to the prior temperature and deformation, all samples were subjected to the following thermal protocol (figure 1). The samples were first heated to 165 °C (which was above the equilibrium melting point of polyethylene, $T_m^o \sim 145.5$ °C) and were held there for 5 min. The equilibrated melt was then rapidly cooled down to the chosen crystallization temperature (112 or 115 °C) at a rate of 30 °C min^{-1}. These crystallization temperatures indicated that the measurements were carried out at a low degree of supercooling (in fact, 112 °C was the nominal peak melting point for both MB-50k and MB-50k/MD-161k (90/10) samples). Once the temperature reached the chosen experimental temperature, a WAXD (or SAXS) pattern was collected before shear to ensure that the residual orientation was indeed removed. The shear rate was 60 s^{-1}, chosen for the following reasons. (1) At a low shear rate, corresponding to a higher critical orientation molecular weight [10–13], no orientation was seen in both MB-50k and Mb-50k/MD-171k (90/10) samples. (2) At a higher shear rate, for example 90 s^{-1}, the intense shear appeared to start distorting the sample shape.

Time-resolved x-ray images were taken upon the cessation of shear (time zero was recorded when shear stopped). The acquisition time for each image was 10 s with an interval of 5 s for data transfer between the adjacent images. The program was set to collect 120 consecutive x-ray images. In each run, an air scattering pattern with no sample between the two windows of the shear stage was also collected. The background correction of the WAXD and SAXS images was performed to eliminate the air scattering background. All x-ray images were corrected for beam fluctuations and sample absorption. The analysis of the x-ray data was carried out using the corrected patterns.

3. Results and discussion

3.1. DSC thermograms

DSC melting thermograms (taken from the second heating scan) from MD-161k, MB-50k and MB-50k/MD-161k blend are illustrated in figure 2. The nominal melting temperature (T_m) and end melting temperature (T_m^{end}) of three samples are listed in table 1, where T_m was taken as the peak temperature of the DSC endotherm and T_m^{end} was taken as the end temperature of the melting curve. The nominal melting point of MD-161k is 108 °C, which is lower than that of typical polyethylene samples with the same molecular weight synthesized by conventional Ziegler–Natta or metallocene methods [31]. This is because the presence of butene units greatly reduces the melting point as well as the degree of crystallinity of MD-161k. It is seen that the melting curves for three samples in figure 2 all exhibit a single

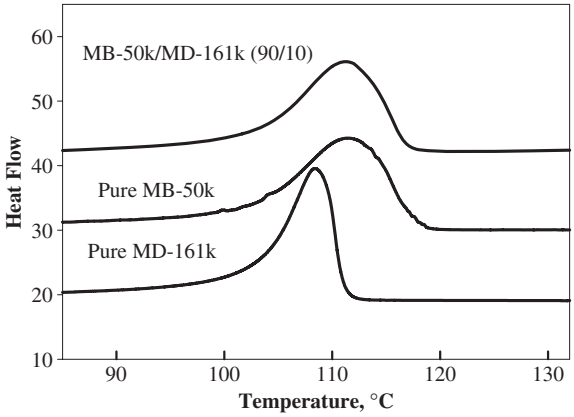

Figure 2. DSC thermograms of MB-50k, MD-161k and MB-50k/MD-161k taken from the second heating scan with a heating rate of 10 °C min^{-1}.

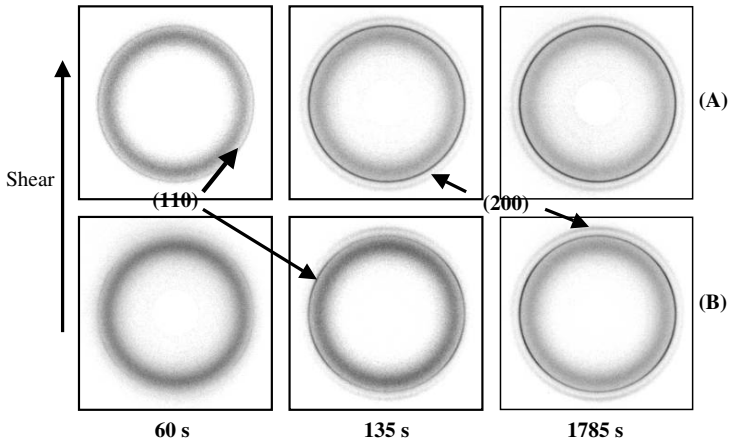

Figure 3. Selected 2D WAXD patterns of (A) MB-50k and (B) MB-50k/MD-161k after shear cessation (shear rate = 60 s^{-1}, shear time = 5 s, temperature = 112 °C).

endotherm. The values of T_m and T_m^{end} for MB-50k and MB-50k/MD-161k blend are almost identical (table 1 and figure 2), indicating that MB-50k and MD-161k are fully miscible after solution blending and the crystallization behaviour of the blend is dominated by the MB-50k component. Since MB-50k and MB-50k/MD-161k (90/10) blends exhibited the same nominal melting point, the crystallization behaviour of these two materials was compared at the same degree of supercooling under both quiescent and flow conditions.

3.2. In situ WAXD after cessation of shear

3.2.1. 2D WAXD results. Selected 2D WAXD patterns of MB-50k and MB-50k/MD-161k blend at 112 and 115 °C at varying times after cessation of shear (shear rate = 60 s^{-1}, shear time = 5 s) are shown in figures 3 and 4, respectively (we note that 112 °C is the nominal melting point of MB-50k and both experimental temperatures were above the nominal melting temperature of MD-161k). 2D WAXD measurements of both MB-50k and MB-50k/MD-161k samples without shear at the same temperatures were also conducted in order to make comparisons (data not shown here as they only exhibited unoriented reflections). It is necessary to briefly describe the quiescent crystallization results from unsheared samples

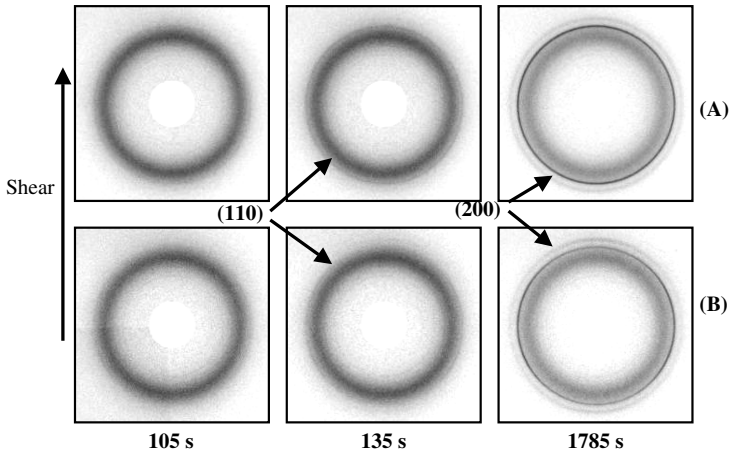

Figure 4. Selected 2D WAXD patterns of (A) MB-50k and (B) MB-50k/MD-161k after shear cessation (shear rate = 60 s^{-1}, shear time = 5 s, temperature = 115 °C).

before we discuss the structure changes after cessation of shear. WAXD patterns from MB-50k quiescently crystallized at 112 and 115 °C exhibited crystallization induction times of 75 and 150 s, respectively. Two crystal reflections were seen—they become stronger with time, but neither exhibited any orientation. Much like the case of MB-50k, the MB-50k/MD-161k blend without shear exhibited the induction times of 60 s at 112 °C and 135 s at 115 °C, respectively.

Figure 3 shows that two crystal reflections were detected at around 60 s after cessation of shear at 112 °C for both MB-50k and MB-50k/MD-161k samples. In the blend, these two reflections were oriented exhibiting distinct azimuthal variation in intensity, whereas in MB-50k, the two reflections were nearly isotropic. These results indicated that the crystal orientation developed in the blend after shear was significantly stronger than that in MB-50k. It was seen that the blend exhibited four arc-like (110) reflections at the off-axis direction and two arc-like (200) reflections on the meridian. This indicates the formation of twisted lamellae, which is a common phenomenon in PE spherulites consisting of lamellar stacks [1, 32]. This observation can be explained as follows. As the folded-chain lamellae grow epitaxially from the *c*-axis of the flow-induced row nuclei, they twist gradually around the crystallographic *b*-axis. In other words, when twisted lamellae occur, the lamellar growth direction becomes aligned with the *b*-axis, where *c*-axis and *a*-axis rotate around the *b*-axis. With the increase in time, the crystalline reflections from both samples grew stronger, indicative of the increase in crystallinity.

The changes in crystalline reflections for the WAXD patterns collected from MB-50k and MB-50k/MD-161k at 115 °C (figure 4) are very similar to that observed at 112 °C, except that the crystallization occurred at a relatively later time for both samples and the orientation in MB-50k/MD-161k appeared to be weaker. It was seen that the (110) reflection started to appear in both samples at 105 s, where the corresponding intensities became substantially weaker than those at 112 °C. Similar to the observations in figure 3, the MB-50k/MD-161k blend exhibited stronger crystal orientation after shear cessation than that of MB-50k.

Figure 5 illustrates the azimuthal intensity profiles taken from the (110) reflection for both samples at 1785 s after shear cessation ((A): 112 °C and (B): 115 °C). It was seen that the azimuthal intensity variation in the MB-50k/MD-161k blend was much more prominent than that in MB-50k at both temperatures. MB-50k was found to exhibit very weak orientation at

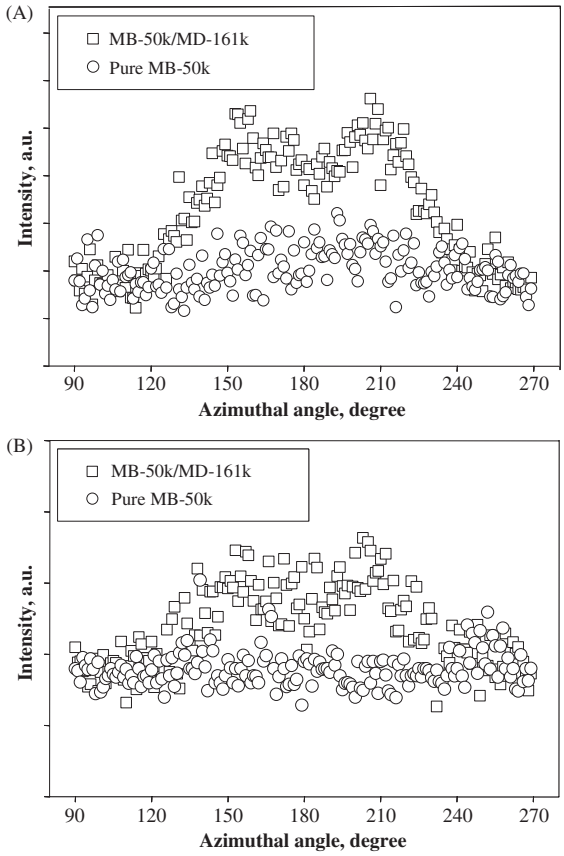

Figure 5. Total azimuthal intensity profiles taken from the (110) reflection of both samples at 1785 s after shear cessation at (A) 112 °C and (B) 115 °C.

112 °C and almost no orientation at 115 °C. Moreover, in the MB-50k/MD-161k blend, the orientation observed at 112 °C was much stronger than that in MB-50k, whereas it decreased slightly at 115 °C. The positions of the two peaks (at around 160° and 210°) in the azimuthal intensity profiles also confirmed the four arc-like (110) pattern at the off-axis direction seen in figures 3 and 4.

3.2.2. Crystallinity changes and crystallization kinetics. Circularly averaged 1D WAXD intensity profiles as a function of scattering angle, 2θ, for the MB-50k/MD-161k blend at various times after shear are shown in figure 6. It is seen that with increasing time, both the (110) ($2\theta = 21.6°$) and (220) ($2\theta = 23.1°$) crystal reflections grew stronger. These profiles also provided the base for calculating the crystallinity index (termed 'crystallinity' hereafter). The procedure for this calculation has been described elsewhere [14].

The evolution of total crystallinity of MB-50k and MB-50k/MD-161k at 112 and 115 °C as a function of time is depicted in figure 7. It was seen that the level of total crystallinity in MB-50k was always higher than that in the blend at both temperatures. For example, at 112 °C, the final values of total crystallinity at the end of experimental time frame were 12% and 8% for MB-50k and MB-50k/MD-161k, respectively. Similarly, at 115 °C, the final value of total crystallinity was 8.5% for MB-50k and 4.5% for the blend. The total crystallinity decreased with increasing crystallization temperature because the mobility of polymer chains increased with temperature. It was further seen that at both experimental temperatures, MB-50k

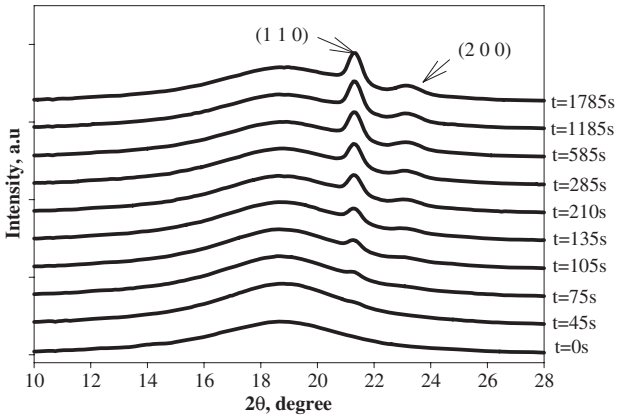

Figure 6. Circularly averaged 1D WAXD intensity profiles as a function of scattering angle of MB-50k/MD-161k at various times after shear cessation. (shear rate = 60 s^{-1}, shear time = 5 s, temperature = 112 °C).

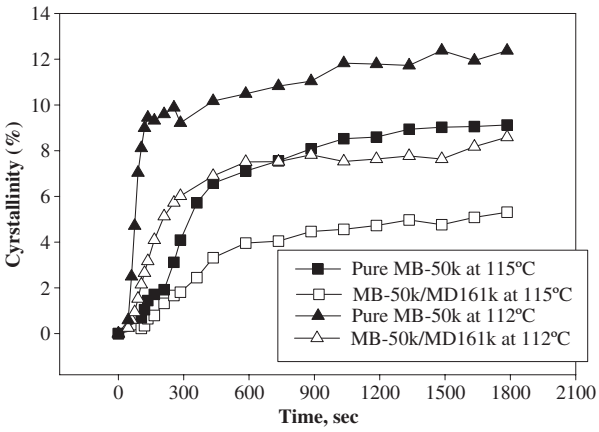

Figure 7. Total crystallinity development in MB-50k and MB-50k/MD-161k at 112 and 115 °C under flow.

exhibited a faster crystallization rate than MB-50k/MD-161k under the same shear condition (shear rate = 60 s^{-1}, shear time = 5 s), which is discussed next.

Figure 8 shows the crystallization half-time ($t_{1/2}$) for both samples at the chosen experimental conditions (shear rate = 60 s^{-1}, shear time = 5 s, T = 112 °C or 115 °C). It was seen that the crystallization half-time values for MB-50K were less than those in MB-50K/MD-161k at both temperatures under the chosen shear conditions. Furthermore, the crystallization half-time values increased with the increase in temperature. These results indicate that MB-50k crystallized faster than MB-50K/MD-161k at both temperatures. Based on the above findings, it can be concluded that the addition of long polymer chains (i.e., 10 wt%MB-161k) to the low molecular weight matrix (MB-50k) lowered the crystallization rate and the total crystallinity but led to much higher degree of crystal orientation under shear.

3.2.3. Crystal orientation in the MB-50k/MD-161k blend. *In situ* WAXD results indicated that MB-50K/MD-161k showed distinct crystal orientation after shear, while MB-50k exhibited almost no orientation (figures 3 and 4). Figure 9 displays the evolution of total crystallinity and oriented crystallinity in MB-50K/MD-161k at both experimental temperatures. The crystallinity due to the oriented fraction was obtained using the WAXD data analysis scheme outlined in a previous publication [14]. It has been noted earlier that the total crystallinity developed at a faster rate at 112 °C than that at 115 °C. This was also seen in the rate of oriented

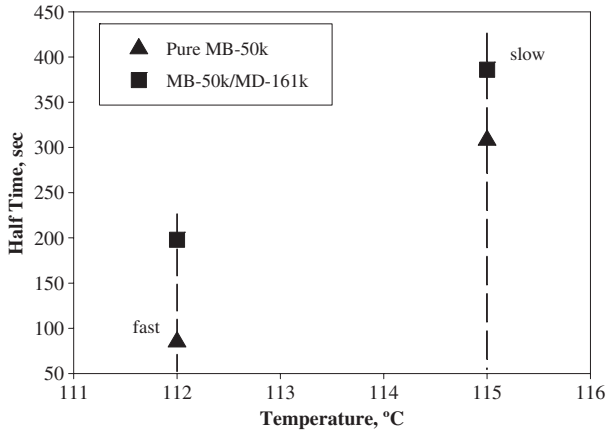

Figure 8. Values of crystallization half-time in MB-50k and MB-50k/MD-161k under flow condition at 112 and 115 °C.

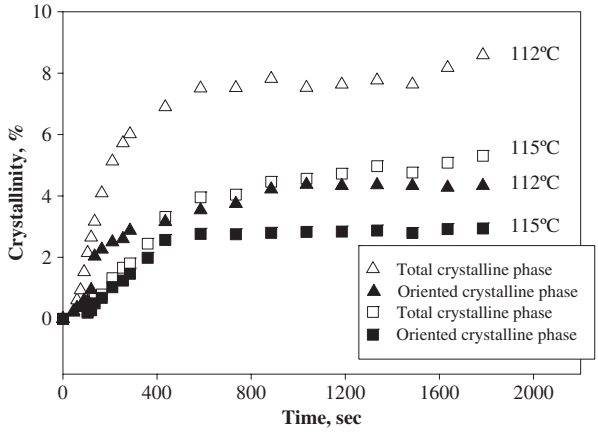

Figure 9. Evolutions of total crystallinity and oriented crystallites in MB-50K/MD-161k at two different temperatures for the blend.

crystallinity development. Furthermore, it was found that in the early stages of crystallization, the oriented crystallinity was nearly equal to the total crystallinity. This indicates that the initially formed crystalline structure was highly oriented. The unoriented crystals started to develop later than the occurrence of oriented crystals, but they became dominant at the later stage of the crystallization process. At the end of crystallization, the oriented crystallinity was about half of the total crystallinity in the blend for both temperatures.

It seems that the only advantage of incorporating MD-161k into the MB-50k matrix is to enhance the degree of crystal orientation. As discussed earlier, Keller *et al* [1] proposed the idea of the critical orientation molecular weight M^* in elongational flow and our group has confirmed this concept in shear flow. This concept can be explained as follows. At a given shear rate, only molecules with a chain length above M^* can remain oriented after deformation, which may lead to formation of primary nuclei that can further induce folded-chain lamellae. Under the selected shear conditions (shear rate $= 60\ s^{-1}$), we confirmed that short MB-50k chains could not stay oriented after shear, since they quickly relaxed back to the random coil state due to short relaxation times. As a result, pure MB-50k exhibited almost no crystal orientation after shear. On the other hand, the addition of MD-161k significantly enhanced the degree of crystal orientation. This can be explained as follows. Longer MD-161k chains could remain in the stretched state after shear due to their longer relaxation times. Subsequent crystallization of the extended chains would lead to the shish structure, which could then induce

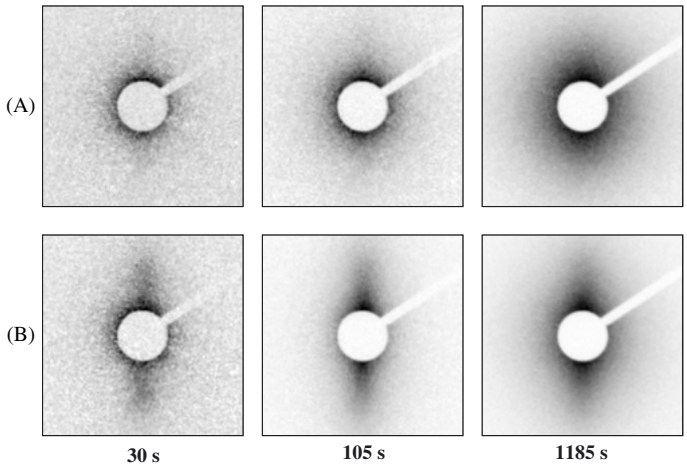

Figure 10. Selected 2D SAXS patterns of (A) MB-50k and (B) MB-50k/MD-161k after shear cessation (shear rate = 60 s^{-1}, shear time = 5 s, temperature = 112 °C).

folded-chain lamellae (i.e., kebabs). It should be noted that not all MD-161k chains could be extended because the entanglement between the polymer chains would greatly reduce the extent of chain extension. As a result, two populations of MD-161k chain segments should be formed: stretched and coiled segments. Therefore, stretched MD-161k chains are mainly responsible for the initial formation of extended-chain crystals (shish or oriented nuclei), whereas coiled MD-161k as well as coiled MB-50k chains are responsible for the formation of folded-chain lamellae (kebabs), which are perpendicularly oriented to the shish.

3.3. In situ SAXS after cessation of shear

3.3.1. 2D SAXS results. Selected 2D SAXS patterns of (A) MB-50k and (B) MB-50k/MD-161k samples at varying times after shear at 112 and 115 °C are shown in figures 10 and 11, respectively. The flow direction in these figures is vertical. Consistent with the WAXD results from MB-50k and MB-50k/MD-161k under no shear, 2D SAXS patterns collected in these measurements exhibited a diffuse ring with scattering maximum but no orientation at both temperatures. The ring scattering feature was due to the formation of a randomly oriented lamellar structure.

It was seen that MB-50k/MD-161k exhibited a strong meridional scattering streak along the flow direction that appeared almost immediately (30 s) after shear (figure 10(B)), while MB-50k exhibited only a weak meridional scattering feature (figure 10(A)). In both samples, these oriented scattering features grew stronger with increasing time. It was clear that orientation developed more quickly in MB-50k/MD-161k than in MB-50k. For instance, at 105 s after cessation of shear, MB-50k/MD-161k already exhibited relatively intense meridional maxima, whereas there was no notable meridional scattering detected in MB-50k. At the end of the experiment (t = 1785 s), the SAXS pattern from the blend exhibited much stronger meridional scattering maxima than that from MB-50k. The meridional scattering maxima in the SAXS pattern could be attributed to the kebab-like lamellar crystals that are oriented perpendicularly to the flow direction. No equatorial streak, which could have been attributed to the shish-like extended-chain structures, was observed in either MB-50k or MB-50k/MD-161k. Similar behaviour has been observed in previous shear-induced crystallization studies in

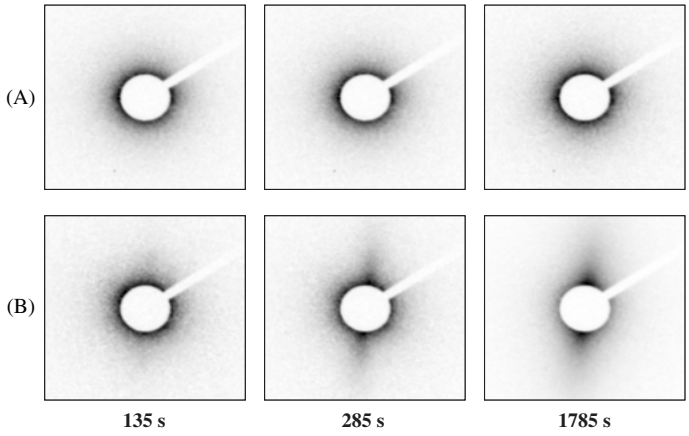

Figure 11. Selected 2D SAXS patterns of (A) MB-50k and (B) MB-50k/MD-161k after shear cessation (shear rate = 60 s^{-1}, shear time = 5 s, temperature = 115 °C).

iPP melt [10, 11]. It is noted that the absence of the equatorial streak does not necessarily mean that the nuclei with shish-like structures did not form; it is also possible that under the chosen shear conditions, the shish were just too small or the concentration was too low to be detected by SAXS.

2D SAXS patterns of (A) MB-50k and (B) MB-50k/MD-161k at selected times after shear (shear rate = 60 s^{-1}, shear time = 5 s) at 115 °C are illustrated in figure 11. It was seen that the SAXS patterns from MB-50k only exhibited a diffuse scattering ring with no orientation after shear during the whole experiment, confirming the absence of any kind of oriented structures. In the blend, the meridional scattering maxima were first observed at 135 s after shear, which was later than the corresponding initial appearance of orientation at 112 °C (figure 10). The last pattern collected at 1785 s after shear cessation at 115 °C showed a less prominent meridional streak in comparison with the similar one at 112 °C.

One interesting feature from the SAXS results is the appearance of a meridional streak instead of a pair of meridional scattering peaks, which was usually seen from SAXS patterns of oriented semicrystalline polymer samples [13]. Such peaks are generally attributed to the formation of oriented lamellar structure having relatively large lateral dimensions, while the meridional streak can arise from the formation of highly oriented lamellar structures with small lateral dimensions and a large polydispersity in their diameter (as in shish-kebabs). Information obtained from these unique meridional streaks will be presented later.

Consistent with the WAXD data, SAXS results indicated that the enhancement of crystal orientation occurred in MB-50k/MD-161k at both temperatures. Again, these results suggest that the initially formed oriented precursor structures, which act as a template for further full-scale crystallization and can greatly improve the total crystal orientation, mainly arise from longer polymer chains. We also note that the orientation shown in SAXS appears to be more pronounced than that shown in WAXD, especially in MB-50k. This is because SAXS could detect any form of the oriented structure (not necessary the crystalline form) as long as there is sufficient density contrast.

3.3.2. Long period between the adjacent lamellae (kebabs). It is well known that the analysis of the long period involves the use of the peak position of the Lorentz corrected profile based on Bragg's law. The changes of long period between the adjacent lamellae in MB-50k and

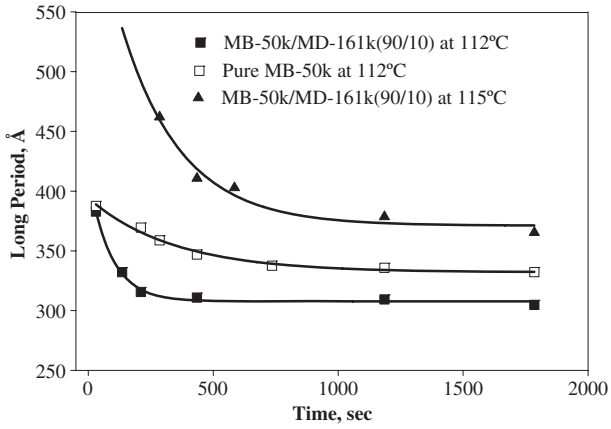

Figure 12. Variation of lamellar long period in MB-50k and MB-50k/MD-161k at 112 and 115 °C as a function of time.

MB-50k/MD-161k as a function of time at two experimental temperatures are shown in figure 12. At 112 °C, the long period slightly decreased in the beginning of crystallization and reached a plateau value afterwards for both samples (in MB-50k, the long period decreased from 388 to 346 Å and remained about constant at $t > 450$ s; in MB-50k/MD-161k, the long period decreased from 383 to 316 Å and remained constant after $t > 210$ s). The slight decrease in the long period can be explained by the formation of new lamellae, probably through the mechanism of lamellar insertion between the established lamellae [1]. It is also seen that the difference between the plateau values of the long period for the two samples was considered to be not significant. Thus, the lamellar structures formed in MB-50k and MB-50k/MD-161k at 112 °C after shear appeared to be quite similar. At 115 °C, the lamellar structures were only developed in MB-50k/MD-161k. It was seen that the average long period was quite large at the beginning of the crystallization (475 Å) and then started to rapidly decrease. Subsequently, for instance when $t > 800$ s, the decreasing rate slowed down and long period reached a plateau with a value of around 380 Å. The large long period at the very beginning of crystallization is possibly due to the formation of loosely ordered lamellar structures under the lower degree of supercooling. It is conceivable that these lamellae may be largely uncorrelated such that Vonk's method can be used to estimate the lamellar thickness, as will be discussed in the following section.

3.3.3. Lamellar thickness estimated using Vonk's method for single lamella scattering. Figure 13 illustrates the sliced SAXS profiles along the meridional direction as a function of s ($s = 2\sin\theta/\lambda$ with θ being the scattering angle and λ being the wavelength) in the blend at selected times and varying temperatures after cessation of shear. It is interesting to note that all scattering profiles exhibited a single decay with no clear sign of first-order interference. Vonk [33] proposed that such scattering profiles could result from the following situation. In a dilute lamellar system, the lamellae are not correlated. The relationship between the lamellar thickness, l, and the scattered intensity, $I(s)$, can be expressed as

$$I(s) = \frac{P\sin^2(\pi ls)}{(\pi ls)^2 s^2} \tag{1}$$

where P is a constant. The sine function in equation (1) can be expanded and approximated as

$$I(s) = \frac{P}{s^2} - \frac{1}{3}\pi^2 l^2 P. \tag{2}$$

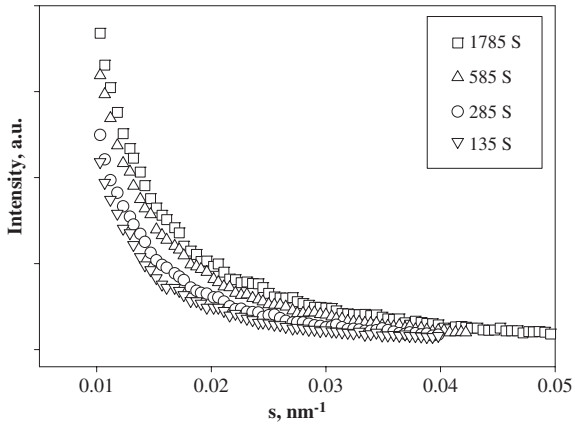

Figure 13. Sliced SAXS profiles for the blend along the meridional direction taken at selected times after shear cessation (shear rate = 60 s^{-1}, shear time = 5 s, temperature = 115 °C), where no first-order interference was observed.

The absence of first-order interference in the SAXS profiles of MB-50k/MD-161k at 115 °C after shear resembles the description of Vonk's scenario. In other words, the sliced meridional profile of the vertical scattering streak may fit the criterion of single lamellar scattering. Figure 14(A) shows the typical plot of $I(s)$ versus $1/s^2$ for the SAXS profile of MB-50k/MD-161k at 285 s after shear at a temperature of 115 °C. A linear fashion of regression was used to determine the average thickness of the kebab, l, based on equation (2). It should be noted that Vonk's method failed to fit the SAXS profiles for either MB-50k or the MB-50k/MD-161k blend at 112 °C after shear. This may be because the lamellar structures formed at a low temperature and they become well correlated along the flow direction. Thus, long period (L), lamellar thickness (l) and amorphous thickness ($l_a = L - l$) are only shown for MB-50k/MD-161k at 115 °C in figure 14(B). Similar to the trend of long period changes with time after shear, the lamellar thickness also slightly decreased in the beginning from 137 to 98 Å and then remained about constant after $t > 900$ s with a value of 75 Å. The change in the interlamellar amorphous layer thickness (l_a) was less than the changes in L and l. The value of l_a only exhibited a small decay in the very beginning and remained about constant at $t > 450$ s.

We can attribute these changes to the following possibility. A secondary crystallization process occurs with the formation of thinner defective lamellar stacks between the existing primary stacks with larger thickness. Similar observations have been reported in other crystalline polymers [34, 35]. Tanzawa *et al* [36] studied the effect of molecular weight on the lamellar thickness of isotactic polystyrene crystallized at high supercoolings from dimethyl phthalate solution. They found that the lamellar thickness increased with molecular weight. They explained this on the basis of loops existing in the molecular conformation in solution. Luo *et al* [37] further confirmed the above relationship between the molecular weight and lamellar thickness based on results of poly(hydroxybutyrate-*co*-hydroxyvalerate) with different molecular weight. They observed that the value of lamellar thickness varied linearly with the molecular weight. Therefore, it is expected that MD-161k could possibly form thicker lamellae than MB-50k. When the shear field is removed, only long polymer chains MD-161k could stay oriented and form the precursor scaffold containing the shish-like extended-chain conformation (may not be detected from SAXS) and folded-chain lamellae. It is likely that only part of MD-161k chains could remain in the stretched state, while the rest would fold and form relatively thicker kebabs. Subsequently, shorter MB-50k chains would also fold and form thinner lamellae. This could result in the decrease in the average lamellar thickness, as observed in our experiments.

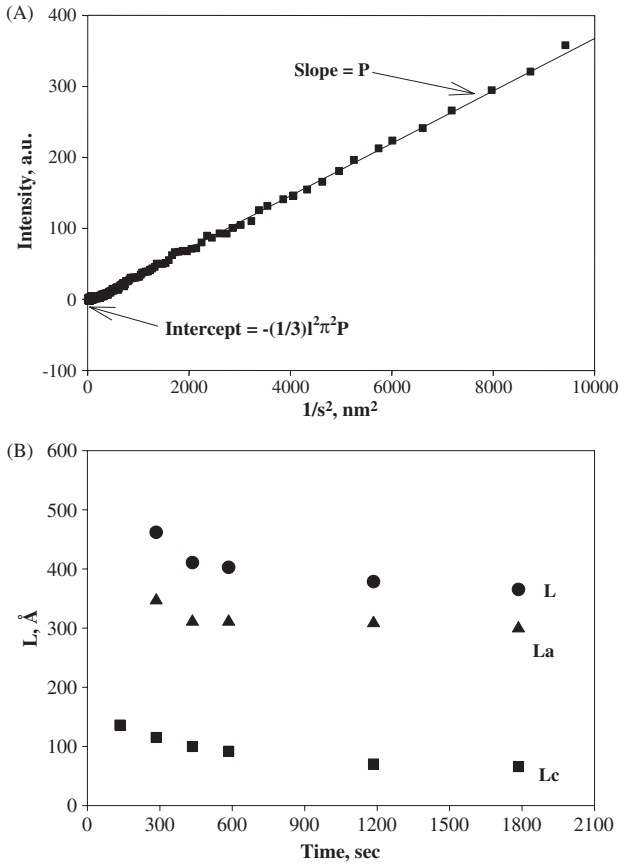

Figure 14. (A) The plot ($I(s)$ versus $1/s^2$) based on Vonk's method for single lamellar scattering for the estimation of lamellar thickness of MB-50k/MD-161k under shear at 115 °C, (B) the changes of calculated lamellar thickness, long period, amorphous layer thickness as a function of time in MB-50k/MD-161k after shear cessation at 115 °C.

4. Conclusions

In situ shear-WAXD and shear-SAXS techniques were utilized to study the nature of the crystallization induced by shear in a model PE blend with a monodisperse, high molecular weight component. Comparisons were made between samples with and without this component in order to illustrate the role of long chains in the flow-induced crystallization. Both WAXD and SAXS results indicated that the presence of the long chains profoundly enhanced the formation of shear-induced precursor structures, which directly led to the higher degree of crystal orientation in the blend. In this study, we clearly showed that longer polymer chains (MD-161k) are mainly responsible for the formation of the precursor scaffold, which further dictate the crystallization and orientation of low molecular weight chains. At experimental temperatures (112 and 115 °C), MB-50k exhibited faster crystallization kinetics and higher crystallinity, possibly due to the high chain mobility in the pure sample with low molecular weight. The lamellar long period in all experimental runs was found to decrease slightly at the beginning of the crystallization process and subsequently reached a plateau value. Vonk's method for single lamella scattering was employed to estimate the lamellar thickness in the

blend at 115 °C, which was found to decrease at the beginning and then remained about constant.

Acknowledgments

We acknowledge the assistance of Dr Carlos A Avila-Orta for synchrotron SAXS and WAXD experimental setup. The financial support of this work was provided by the National Sciences Foundation (DMR-0405432) and ExxonMobil Chemical.

References

[1] Keller A and Kolnaar H W 1997 *Mater. Sci. Technol.* **18** 189
[2] Ziabicki A 1976 *Fundamentals of Fiber Formation* (New York: Wiley)
[3] Eder G and Janeschitz-Kriegl H 1997 *Mater. Sci. Technol.* **18** 268
[4] Lee O and Kamal M R 1999 *Polym. Eng. Sci.* **39** 236
[5] Ward I M 1975 *Structure and Properties of Oriented Polymers* (New York: Wiley)
[6] Bassett D C 2001 *Proc. Int. Conf. on Flow Induced Crystallization of Polymers (Salerno, Italy)* p 59
[7] Garcia Gutierrez M-C, Alfonso G C, Riekel C and Azzurri F 2004 *Macromolecules* **37** 478
[8] Li L and de Jeu W H 2004 *Macromolecules* **37** 5646
[9] Strobl G 2000 *Eur. Polym. J.* E **3** 165
[10] Nogales A, Hsiao B S, Somani R H, Srinivas S, Tsou A H, Balta-Calleja F J and Ezquerra T A 2001 *Polymer* **42** 5247
[11] Somani R H, Hsiao B S, Nogales A, Srinivas S, Tsou A H, Sics I, Balta-Calleja F J and Ezquerra T A 2000 *Macromolecules* **33** 9385
[12] Somani R H, Hsiao B S, Nogales A, Fruitwala H, Srinivas S and Tsou A H 2001 *Macromolecules* **34** 5902
[13] Somani R H, Yang L, Hsiao B S, Agarwal P K, Fruitwala H A and Tsou A H 2002 *Macromolecules* **35** 9096
[14] Yang L, Somani R H, Scis I, Hsiao B S, Kolb R, Fruitwala H and Ong C 2004 *Macromolecules* **37** 4845
[15] Hsiao B S, Yang L, Somani R H, Avila-Orta C A and Zhu L 2005 *Phys. Rev. Lett.* **94** 117802
[16] Somani R H, Yang L, Hsiao B S, Zhu L and Hsiao B S 2005 *Polymer* **46** 8587 (feature article)
[17] Somani R H, Yang L, Hsiao B S and Fruitwala H 2003 *J. Macromol. Sci. Phys.* B **42** 515–31
[18] Bashir Z, Odell J A and Keller A 1972 *J. Mater. Sci.* B **6** 493
[19] Jerschow P and Janeschitz-Kriegl H 1997 *Int. Polym. Process.* **12** 72
[20] Thurman D W, Fernandez-Ballester L, Oberhauser J P and Kornfield J A 2004 *PMSE Preprints* **91** 316–7
[21] Seki M, Thurman D W, Oberhauser J P and Kornfield J A 2002 *Macromolecules* **35** 2583
[22] Lagasse R R and Maxwell B 1976 *Polym. Eng. Sci.* **16** 189
[23] Duplay C, Price F and Stein R 1978 *J. Polym. Sci. (Polym Symp.)* **63** 77
[24] Vleeshouwers S and Meijer H 1996 *Rheol. Acta* **35** 391
[25] Hu W, Frenkel D and Mathot V B F 2002 *Macromolecules* **35** 7172
[26] Dukovski I and Muthukumar M 2003 *J. Chem. Phys.* **118** 6648
[27] Wang M, Hu W, Ma Y and Ma Y Q 2005 *Macromolecules* **38** 2806
[28] Avila-Orta C A, Burger C, Somani R H, Yang L, Marom G, Medellin-Rodriguez F J and Hsiao B S 2005 *Polymer* **46** 8859
[29] Keum J K, Burger C, Hsiao B S, Somani R H, Yang L, Chu B, Kolb R, Chen H and Lue C-T 2005 *Prog. Colloid Polym. Sci.* **130** 1–13
[30] Zuo F, Keum J K, Yang L, Somani R H and Hsiao B S 2006 *Macromolecules* **39** 2209–18
[31] Howard P R and Crist B 1989 *J. Polym. Sci., Polym. Phys. Ed.* **27** 2269
[32] Nadkarni V M and Schultz J M 1977 *J. Polym. Sci., Polym. Phys. Ed.* **15** 2151
[33] Vonk C G 1985 *J. Polym. Sci., Polym. Phys. Ed.* **23** 2539
[34] Hsiao B S, Wang Z, Yeh F, Yan G and Sheth K C 1999 *Polymer* **40** 3515
[35] Ezquerra T A, Lopez-Cabarcos E, Hsiao B S and Balta-Calleja F J 1996 *Phys. Rev.* E **1** 989 (brief report)
[36] Tanzawa, Miyaji H, Miyamoto Y and Kiho H 1988 *Polymer* **29** 904
[37] Luo S, Grubb D T and Netravali A N 2002 *Polymer* **43** 4159